Conference Proceedings

743

XAS investigation on polyvalent cation intercalation in V_2O_5 aerogels

a

Marco Giorgetti,[a] Stefano Passerini,[a]* Mario Berrettoni[b] and William H. Smyrl[a]

[a]Corrosion Research Center, Chemical Engineering and Materials Science Department, University of Minnesota, Minneapolis MN 55455, USA [b]Chemistry Department, University of Camerino, 62032 Camerino, . Email:passerin@cems.umn.edu

In this report are presented the results of XAS investigations on zinc intercalated V_2O_5. EXAFS spectra recorded at the Zn k-edge showed differences in the first shell of intercalated Zn^{2+} as the concentration increased. The interaction of zinc ions with the surrounding V_2O_5 aerogel structure is discussed as well.

Keywords: XAS; intercalation; V_2O_5 aerogel.

1. Introduction

Vanadium pentoxide, gel-based materials have been widely investigated as cathode materials for rechargeable lithium batteries (Livage, 1991). Recently, it has been shown that the aerogel form (later called ARG) has superior properties as an intercalation host for lithium as well as for polyvalent cations. Up to four equivalents of cation (Li^+, Mg^{2+}, Zn^{2+}, Al^{3+}) per mole of V_2O_5 can be reversibly intercalated into the ARG (Le et al., 1996; Le et al., 1998). To characterize the structure of the ARG, XAS investigations were performed on lithium intercalated samples (Passerini et al., 1997). Surprisingly, the lithium intercalation in V_2O_5 aerogels was found to leave the oxidation state of the vanadium ions unaffected. These results, in contrast with experimental results obtained for crystalline V_2O_5 (Cartier et al. 1990) and xerogels (Passerini et al. 1996), clearly indicated the unique nature of the ARG structure.

The characterization of the ARG structure to reveal the nature of the cation intercalation process is the objective of the present work. Since ARGs are mostly amorphous materials (Le et al., 1996; Passerini et al., 1997), the investigations were carried out by means of XAS. The introduction of a second internal structural probe, zinc, into the material has been successful and has helped to improve the understanding of the V_2O_5 aerogel structure as well as of the cation intercalation process.

2. Experimental

Vanadium pentoxide hydrogels were synthesized by ion exchange processing of sodium metavanadate (Livage, 1992; Le et al., 1996). Aerogels were obtained using the procedure described by Le et al. (1996).

Chemical intercalation of the aerogel was carried out at room temperature by reaction with dimethyl zinc (Aldrich) in heptane. A complete description of the procedure used is given in Le et al. (1998). Chemically intercalated $Zn_xV_2O_5$ with x= 0.14, 0.52 and 0.72 were prepared.

The pellet samples for the XAS measurements were prepared by mixing the $Zn_xV_2O_5$'s with boron nitride (90%) and then by pressing the mixture at 1 metric ton. The thickness of the pellets was adjusted to produce an absorption (μx) of about 1.

XAS measurements were carried out in transmission mode at the D21 experimental station of the LURE DCI storage ring (Orsay, France) with a positron beam of 1.85 GeV and a maximum current of 310 mA. XANES spectra at the Zn K-edge were carried out with 0.3 eV steps in the 9610-9740 energy range and with an integration time of 4 seconds. EXAFS spectra at the Zn K-edge were collected at 2 eV steps and with an integration time of 8 seconds in the 9550-10450 eV energy range. Energy calibration was carried out before and after every XANES measurement using a 10 μm thick foil of zinc (9659 eV). All measurements were performed at room temperature and under anhydrous conditions.

3. Results

The Zn K-edge XANES spectra (not shown) indicate the absence of any shift of the edge upon increasing amounts of zinc in $Zn_xV_2O_5$. In Figure 1 the EXAFS measurements of the $Zn_xV_2O_5$ samples are illustrated as a k^2-weighted EXAFS plot and the relative Fourier Transform (FT) plot. The figure clearly shows that the EXAFS signals collected from the compounds with x=0.14 and 0.52 were very similar. The only difference, apart from a more pronounced noise at high k values, resides in the amplitude of the EXAFS oscillations.
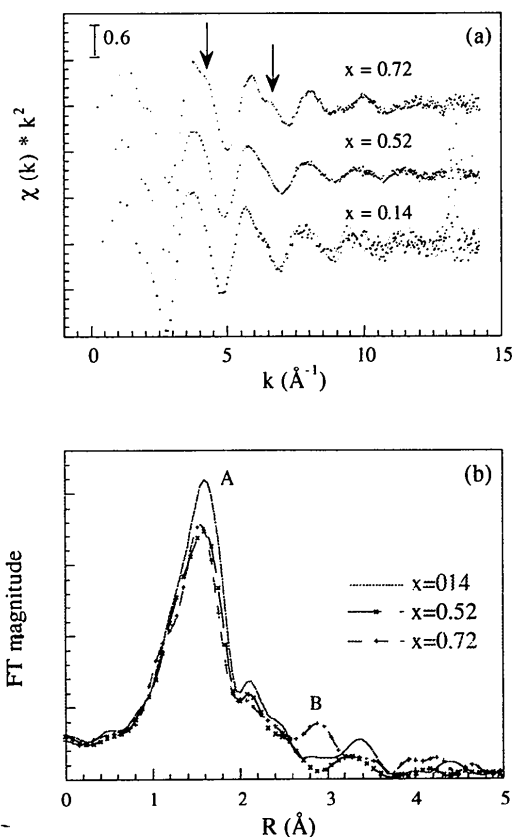
Figure 1
Experimental k^2-weighted EXAFS signals (panel a) and relative FT (panel b) of $Zn_xV_2O_5$ samples at Zn V-edge. The values of x are indicated in the figure

This is also shown by the intensity of the A peaks in panel **b** (FT plot). The EXAFS spectrum of $Zn_{0.72}V_2O_5$ is characterized by new features evident in panel **a**, around $k = 4$ and 6 $Å^{-1}$. They appear as a new peak (B) in the corresponding FT plot (panel **b**), indicating the establishment of new interactions in the material.

Table 1
Results of the EXAFS fitting for $Zn_xV_2O_5$ compounds.

x in $Zn_xV_2O_5$	0.14	0.52	0.72
R Zn-O / Å degeneracy = 4	2.059	2.034	2.014
σ^2 Zn-O / $Å^2$	0.0071	0.0091	0.0087
θ Zn-O-V / deg	94	93	95
R Zn–Zn / Å degeneracy = 2			3.24
σ^2 Zn--Zn / $Å^2$			0.016

4. Discussion

Two different models have been proposed for the ordered layer structure of gel-based V_2O_5 materials. The older one, proposed by Legendre et al. (1983) was directly derived from the structure of crystalline V_2O_5. The second model, introduced by Yao et al. (1992) proposes that each V_2O_5 layer is constituted by two facing $VO_{1.5}$ sheets further sandwiched by two layers of apical oxygens (one oxygen per $VO_{1.5}$ in each layer). Both proposed models satisfy the observed X-ray diffraction data in the reflection mode, i.e., the *00l* class of reflections (Liu et al. 1995). Although the second model appears to give a more accurate estimation of the material density (Yao et al. 1992), some uncertainty on the gel-based V_2O_5 structure remains. Nevertheless, both models predict the presence of co-planar apical oxygens on each side of the layers and in approximately similar positions. Since the purpose of the present work is to characterize the interactions between the intercalated ions and the apical oxygens, the uncertainty on the structural model does not affect the results.

The XANES measurements of the intercalated materials did not show any chemical shift which indicates that the effective charge of the Zn ions is similar in all compounds. This indicates that the zinc site does not change dramatically upon increasing insertion levels of zinc. The bond length and the local environment are maintained.

The EXAFS FT signals of the compounds are characterized by an amplitude decrease of the first peak for increasing amounts of inserted zinc. The same behavior has been commonly seen in intercalated layered materials. It was associated with an increased distribution of the interatomic distances with increasing intercalation level that leads to an increase of the Debye-Waller factor (Ammundsen et al., 1996).

The analysis of the EXAFS measurements was performed by using the GNXAS package (Filipponi et al. 1995; Filipponi & Di Cicco 1995) that takes into account multi-scattering (MS) effects. The measurements were initially analyzed by using the fractional coordinates proposed by Oka et al. (1996) for σ-$Zn_{0.25}V_2O_5 \cdot H_2O$ xerogel. However, the data analysis based on such a model did not give good results for our compounds. In particular, the values of the Zn-O-V angle and

the degeneracy of the Zn-O first shell reported for σ-$Zn_{0.25}V_2O_5 \cdot H_2O$ did not match the experimental results reported in Figure 1. Furthermore, the feature seen in the spectrum of $Zn_{0.72}V_2O_5$ (Figure 1 panel **b**) could not be explained with the structural model given for σ-$Zn_{0.25}V_2O_5 \cdot H_2O$.

To interpret the EXAFS results of $Zn_xV_2O_5$, a four-fold coordination of the zinc ions as well as the existence of a Zn-Zn interaction in $Zn_xV_2O_5$ aerogels was then hypothesized. As customary in EXAFS analysis, the proposed structural model was verified by fitting the experimental curves (Figure 1) to it. The following two- and three-atom contributions were included in the fitting procedure: $\gamma^{(2)}$ Zn-O (first shell), $\gamma^{(2)}$ Zn-O (second shell) and $\eta^{(3)}$ Zn-O-V. In the case of $Zn_{0.72}V_2O_5$, the $\gamma^{(2)}$ Zn-Zn was included as well.
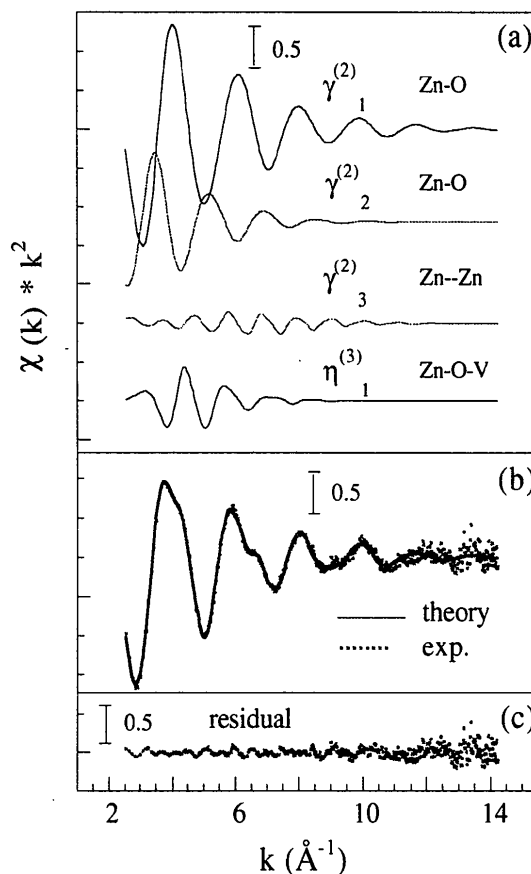
Figure 2
Comparison of the theoretical and experimental signals of the k^2-weighted EXAFS data for $Zn_{0.72}V_2O_5$. Panel **a** shows the individual contributions of the different MS signals; **b** the total theoretical (-) and experimental (...) k^2-weighted EXAFS signals and **c** the residual.

The most relevant results of the fit procedure are reported in Table 1. As an example, the results obtained for $Zn_{0.72}V_2O_5$ are graphically illustrated in Figure 2. The theoretical curve matched the experimental one well and the computed residual was rather low. Both results support the goodness of fit for the structural model herein proposed. The zinc ions are four-fold coordinated by four, co-planar oxygens as indicated by the degeneracy of the Zn-O pair contribution and the value of the Zn-O-V angle. The compound $Zn_{0.72}V_2O_5$, in which more than

50% of the available sites for zinc were occupied, showed the presence of a Zn-Zn interaction due to zinc ions located in adjacent sites.

5. Conclusions

The XAS characterization of zinc intercalated ARGs has shown that in completely anhydrous conditions, the Zn^{2+} ions are four-fold coordinated by four apical oxygens of V_2O_5. Of further importance, the four oxygens belong to the same V_2O_5 layer and the Zn^{2+} ions are located in quasi co-planar positions with them. With the Zn^{2+} ions being almost within a single V_2O_5 layer, the space between two adjacent layers is left almost free even when all the insertion sites available are occupied ($Zn/V_2=1$). The empty interlayer spacing is then available for further ion insertion that explains the large intercalation capacity.

References

Ammundsen, B., Jones, D.J., Rozière, J.,& Burns, G.R. (1996). Chem. Mater. 8, 2799-2808.

Cartier, C., Tranchant, A., Verdaguer, M., Messina, R., Dexpert, H. (1990) Electroch. Acta 35, 889-898.

Filipponi, A., Di Cicco, A. & Natoli, C.R. (1995). Phys. Rev. B 52, 15122-15134.

Filipponi, A. & Di Cicco, A (1995). Phys. Rev. B , 52, 15135-15149.

Le, D.B., Passerini, S., Guo, J., Ressler, J., Owens, B.B., Smyrl, W.H. (1996). J. Electroch. Soc. 143, 2099-2104.

Le, D.B., Passerini, S., Coustier, F., Guo, J., Soderstrom, T., Owens, B.B., Smyrl, W.H. (1998). Chem. Mater. 10, 682-684

Legendre, J.J., Livage, J. (1983) J. Colloid Interface Sci., 94, 75-83.

Livage, J. (1991). Chem. Mater. 3, 578-593.

Liu, Y.J., Cowen, J.A., Kaplan, T.A., DeGroot, D.C., Schindler, J., Kannewurf, C.R., Kanatzidis, M.G. (1995). Chem. Mater. 7, 1616-1624.

Oka, Y., Tamada, O., Yao, T. & Yamamoto, N. (1996). J. Solid State Chem. 126, 65-73.

Passerini, S., Smyrl, W.H., Berrettoni, M., Tossici, R., Rosolen, M., Marassi, R. & Decker, F. (1996). Solid State Ionics, 90, 5-14.

Passerini, S., Le, D.B., Smyrl, W.H., Berrettoni, M., Tossici, R., Marassi, R. & Giorgetti, M. (1997). Solid State Ionics, 104, 195-204.

Yao, T., Oka, Y., Yamamoto, N. (1992) Mat. Res. Bull., 27, 669-675.